APPLICABILITY OF A PORTABLE PARTICLE MONITOR FOR MEASURING TSP AND PM10 IN THE AMBIENT ENVIRONMENT

A Thesis

by

MINGQI ZOU

Submitted to the Office of Graduate and Professional Studies of
Texas A&M University
in partial fulfillment of the requirements for the degree of

MASTER OF SCIENCE

Chair of Committee,	Ronald E. Lacey
Committee Members,	Raghupathy Karthikeyan
	Maria King
Head of Department,	Steve Searcy

May 2017

Major Subject: Biological and Agricultural Engineering

ABSTRACT

The National Ambient Air Quality Standard (NAAQS) was established and revised to regulate PM10 (particles less than or equal to 10 μm in aerodynamic diameter), as these small particles were found to penetrate and deposit in human respiratory tract, causing adverse health effects. The FRM and FEM sampler designated by the USEPA to monitor PM10 and Total Suspended Particles (TSP) mass concentration require either expensive equipment or tedious tests. In many cases, a faster and easier measurement is desired. The goal of this study was to test the applicability of a handheld particle monitor (Aerocet 831, Met One Instruments, Grants Pass, OR) for monitoring PM10 and TSP in the ambient air. This monitor is capable of measuring PM10 and TSP mass concentration in just one minute. To achieve this goal, monodisperse solid ammonium fluorescein aerosols of aerodynamic diameter 3, 5, 7, 9, 10, 11, 13, 15, and 17 μm were generated and introduced into wind tunnel at speed of 2, 8 and 24 km/h. The Aerocet 831 and an isokinetic (reference) air sampler were co-located in the wind tunnel to monitor and collect aerosols simultaneously. Separate tests were performed to find out a mathematical correlation equation between fluorescence intensity unit (FIU) and a wide range of fluorescein particle mass (0-240 μg). The FIU of the particles deposited on filter of isokinetic sampler in each wind tunnel test was measured and converted to particle mass using the correlation equation. Then the sampling effectiveness values were obtained, corrected and fitted to lognormal distribution curves. The Aerocet 831 is suggested having good performance for

monitoring PM10 at wind speed of 2 km/h, however its applicability for measuring PM10 at 8 and 24 km/h is limited due to the oversampling at small particle sizes. It is expected for the Aerocet 831 to be able to monitor TSP in a size range of 0 to 50 μm, but the maximum particle size detection of Aerocet 831 shown from the TSP sampling effectiveness curves is only about 23 μm.

ACKNOWLEDGEMENTS

I would first like to express my sincere appreciation specifically to my committee chair, Dr. Lacey, and to my committed members Dr. King and Dr. Karthi, for their guidance and support throughout this study.

I am obliged to send my thankfulness to Dr. Kalbasi for his teaching and helping on the operation of this project.

Finally, I want to show my profound gratitude to my parents and friends for providing me with continuous encouragement and support in my life.

CONTRIBUTORS AND FUNDING SOURCES

Part 1, Faculty committee recognition

This work was supervised by a thesis committee consisting of Dr. Lacey and Dr. Karthi of the Department of Biological and Agricultural Engineering and Dr. King of the Department of Mechanical Engineering.

Part 2, Student/collaborator contributions

The experiments were conducted in part by Dr. Kalbasi who works as research engineer and scientist in the Department of Biological and Agricultural Engineering. All other work conducted for the thesis was completed by the student independently.

Funding was provided by the Cotton Foundation to support this research.

TABLE OF CONTENTS

Page

ABSTRACT ii

ACKNOWLEDGEMENTS iv

CONTRIBUTORS AND FUNDING SOURCES v

TABLE OF CONTENTS vi

LIST OF FIGURES viii

LIST OF TABLES ix

CHAPTER I INTRODUCTION 1

PM10 and TSP Measurements 2
Objective 7

CHAPTER II EQUIPMENT AND PROCEDURES 9

Equipment 9
Wind Tunnel 9
Vibrating Orifice Aerosol Generator 13
Isokinetic Air Sampler 16
Fluorometer 18
Procedures 19
Solid Ammonium Fluorescein Particle Generation 19
Correlation between Fluorescein Mass and FIU 21
Aerosol Sampling 24

CHAPTER IV RESULTS, DISCUSSION AND CONCLUSION 26

Sampling Effectiveness of Aerocet 831 26
Curve Fitting and Mutiplet Correction 30
Conclusion 36

REFERENCES 38

APPENDIX A PARTICLE SIZE DISTRIBUTION 40

APPENDIX B EXPECTED MASS CONCENTRATION OF AEROCET 831 AT WIND SPEED OF 2 KM/H 44

APPENDIX C EXPECTED MASS CONCENTRATION OF AEROCET 831 AT WIND SPEED OF 8 KM/H 47

APPENDIX D EXPECTED MASS CONCENTRATION OF AEROCET 831 AT WIND SPEED OF 24 KM/H 50

LIST OF FIGURES

Page

Figure 1. Fractional penetration of thoracic aerosols and sampling effectiveness curve of ideal PM10 sampler (Faulkner *et al.*, 2014). 3

Figure 2. Met One Model Aerocet 831 (Met One Instruments, Inc., 2014). 6

Figure 3. Basic light scattering system for counting particles in the air (Yi *et al*., 2015). 7

Figure 4. Schematic of TAMU wind tunnel, VOAG system and sampling system. 10

Figure 5. Position of 33 sampling points for wind velocity measurement (Faulkner *et al*., 2014). 12

Figure 6. Three different nozzles of isokinetic air sampler. 17

Figure 7. Location of isokinetic air sampler and Aerocet 841 inside wind tunnel. 18

Figure 8. Plot of FIU as a function of fluorescein mass for 5μm fluorescein particle. 24

Figure 9. Calculation example of the corrected sampling efficiency for generated test aerosols with multiplets and satellites (Faulkner *et al*., 2014). 31

Figure 10. PM10 sampling effectiveness curves with multiplet correction at wind speed of 2, 8 and 24 km/h. 32

Figure 11. TSP sampling effectiveness curves with multiplet correction at wind speed of 2 and 8 km/h. 33

LIST OF TABLES

Page

Table 1. Performance requirement of wind tunnel for PM10 sampler (40 CFR 53.42). 11

Table 2. Wind velocity uniformity test results (Faulkner *et al*., 2014). 12

Table 3. The composition of solid ammonium fluorescein particle solutions of aerodynamic diameters 3, 5, 7, 9, 10, 11, 13, 15, 17 µm. 16

Table 4. The VOAG frequency adjusted to produce particles of nominal sizes 3, 5, 7, 9, 10, 11, 13, 15, 17 µm, and their corresponding APS volume mean diameter and calculated aerodynamic diameter. 21

Table 5. Different fluorescein mass collected from 5 µm fluorescein solution and their corresponding FIU values. 22

Table 6. Sampling effectiveness results of Aerocet 831 at 2, 8 and 24 km/h. 27

Table 7. Cut-point and slope of lognormal corrected sampling effectiveness curves at 2, 8 and 24 km/h. 34

Table 8. Expected mass concentration of Aerocet 831 based on its PM10 sampling performance at three wind speeds. 35

Table 9. Size distribution of particles of nominal sizes 3, 5, 7, 9, 10 µm generated from wind tunnel tests. 40

Table 10. Size distribution of particles of nominal sizes 10, 11, 13, 15, 17 µm generated from wind tunnel tests. 43

Table 11. Expected mass concentration for Aerocet 831 and ideal PM10 sampler at wind speed of 2 km/h. 44

Table 12. Expected mass concentration for Aerocet 831 and ideal PM10 sampler at wind speed of 8 km/h. 47

Table 13. Expected mass concentration for Aerocet 831 and ideal PM10 sampler at wind speed of 24 km/h. 50

CHAPTER I

INTRODUCTION

Particulate matter (or aerosol) is the sum of all solid and liquid particles suspended in air. Depending on the source, PM can be categorized as a primary aerosol or a secondary aerosol. Primary aerosols are emitted directly from natural sources to the atmosphere, while secondary aerosols are formed from reactions between atmospheric gases and chemicals released from anthropogenic sources (such as power plants, automobile emissions, industrial factories, and concentrated agricultural facilities) (McMurry *et al*., 2004). The National Ambient Air Quality Standard (NAAQS) was first established by the USEPA for total suspended particulates (TSP) under the Clean Air Act in 1971 to protect public health and welfare. It was significantly revised in 1987 when a PM10 standard was formally established to regulate particles less than or equal to 10 μm in aerodynamic diameter at the level of 150 $\mu g/m^3$ for 24 hours averaging time. These smaller particles were found to penetrate and deposit in the tracheobronchial and alveolar regions of the respiratory tract, causing serious health problems. Numerous epidemiological studies have discovered a strong relationship between PM10 and health disorders including short-term (e.g. premature mortality, hospital admissions) and long-term (e.g. morbidity, lung cancer, cardiovascular and cardiopulmonary diseases) (Valavanidis *et al*., 2008). Research has shown that a 10 $\mu g/m^3$ increase of PM10 is associated with a 0.5-1.5% increase in daily mortality (Schwartz, J., 1994). Therefore, PM10 is one of the major air pollution components that threatens both people's health

and environment. Though TSP is no longer considered as the criteria pollutant in NAAQS following the 1987 revision, it was reported that high TSP levels could influence light and heat energy transmission through the atmosphere, and thus affect the earth's radiation balance that controls climate (Davidson *et al*., 2005).

PM10 and TSP Measurements

To comply with the NAQQS criteria for PM10, the 24-hour integrated PM10 concentration from an emission source must not exceed the standard (150 $\mu g/m^3$). Designated PM10 monitors must meet specific standards to be used for regulatory purpose. In 40 Code of Federal Regulations (CFR) 53.43, the USEPA defined the sampling effectiveness curve (effectiveness versus aerodynamic particle size) for ideal PM10 sampler, based on the fractional penetration of thoracic aerosol in human respiratory tract (ISO, 1995) (Faulkner *et al.*, 2014) (Figure 1).

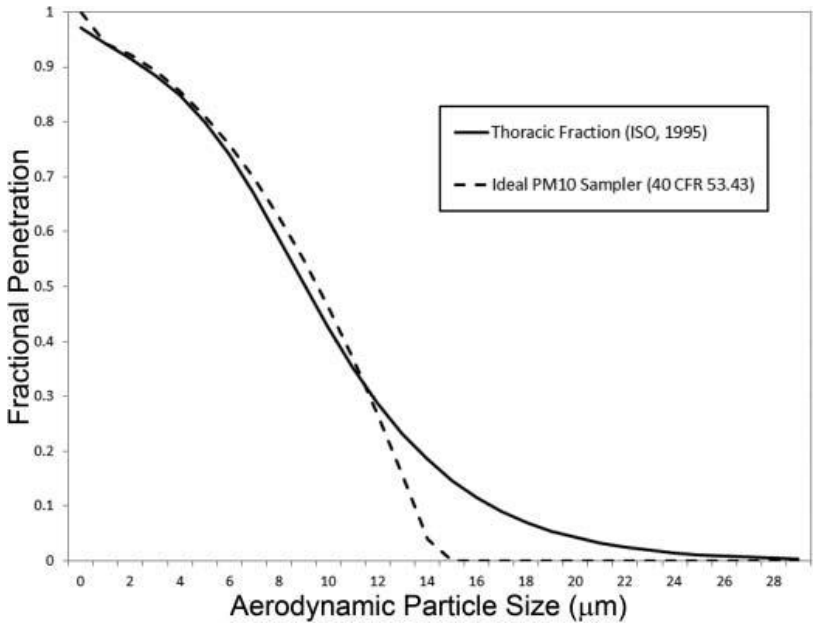

Figure 1. Fractional penetration of thoracic aerosols and sampling effectiveness curve of ideal PM10 sampler (Faulkner *et al.*, 2014).

Samplers must be tested in a wind tunnel and meet the following four requirements before they can be approved by the USEPA as Federal Reference Method (FRM) or Federal Equivalent Method (FEM) sampler (40 CFR 53.40):

1) The sampling effectiveness of the candidate sampler is tested in a wind tunnel at ten specific monodisperse particle with their sizes ranging from 3 ± 0.5 to 25 ± 1.0 μm in aerodynamic diameter at wind speeds of 2, 8, and 24 km/h.
2) The sampling effectiveness curve at each wind speed is determined by fitting a smooth curve to the test data.
3) The 50% cut-point (the point on the performance curve where 50% effectiveness is achieved) is within 10 ± 0.5 μm;

4) The expected mass concentration (of solid particles) for candidate sampler is within ± 15% of that predicted for the ideal sampler (40 CFR 53 Table D-3);

All currently approved FRM and FEM samplers operate on the principle of impaction governed by Stokes' Law and the determination of PM10 mass concentration is based on the weight mass accumulation on either a filter or the shift in vibration of an oscillating tapered element, and the volume of air drawn through the sampler over the sampling time.

Concerns have been raised that FRM PM10 samplers exhibit concentration measurement errors when collecting particles in an environment where the mass median diameter (MMD) is larger than 10 µm (Buser *et al*., 2007). Particulate matter from many agricultural sources typically have a particle size distribution with MMD between 10 and 20 µm and a geometric standard deviation (GSD) ranging from 1.5 to 2.0 (Wanjura *et al*., 2005). One challenge with gravimetric samplers such as the FRM TSP sampler is maintaining constant airflow during the sampling period. Airflow is generally measured with an orifice meter where the pressure differential across the orifice is recorded and the airflow calculated from the Bernoulli equation and the psychrometric properties of the ambient air. Measurement of the pressure differential was shown to be the single largest contributor to the combined measurement uncertainty (Lacey and Faulkner, 2015).

There are portable particle counters available in the market. These units are intended for indoor monitoring with calm air and are used for determining personal exposure to PM. The relative low cost and ease of use of these monitors make them attractive to "citizen scientists" seeking to monitor environmental conditions in specific locations of interest (Dr. Phillip J Wakelyn, personal communication, August 25, 2016). However, there are no data to establish the performance of these instruments in an environment outside of their design specifications.

Met One Instruments (Grants Pass, Oregon) manufactures devices for monitoring particles in both indoor and outdoor environments. Many of their models have been designated by the USE PA as federal reference and equivalent methods, including BAM-1020 Beta Attenuation Mass Monitor (PM2.5 and PM10), BAM PLUS Beta Attenuation Mass Monitor (PM10), BAM-1022 Real Time Beta Attenuation Mass Monitor (PM2.5) and E-FRM (PM2.5). They manufacture a portable particle monitor Aerocet 831 (Figure 2) (Met One Instruments, Inc., 2014), designed for monitoring indoor particles, which is specified to operate at flow rate of 2.83 L/min. The inlet nozzle diameter of Aerocet 831 is about 1.1 cm, so the wind speed at the inlet nozzle is very close to 2 km/h.

Figure 2. Met One Model Aerocet 831.

The Aerocet 831 is a right-angled laser scattering particle counter where particles intersect the laser beam and scatter the light with an amplitude dependent on particle size based on Rayleigh and Mie scattering theory. The scattered light is collected over a wide angle perpendicular to the airflow and laser beam and focused onto a photodiode (Figure 3). The photodiode converts the scattered light signal to an electrical pulse where the amplitude is related to the particle size. An algorithm is used to convert the size of each detected particle to its volume, and a standard density value, which can be adjusted by an empirically derived factor in the instrument software, is used to convert particle volume

to particle mass. The Aerocet 831 reports five mass ranges (µg/m^3): PM1, PM2.5, PM4, PM10 and TSP, in one minute. It has an accuracy of ± 10% and sensitivity of 0.3 µm.

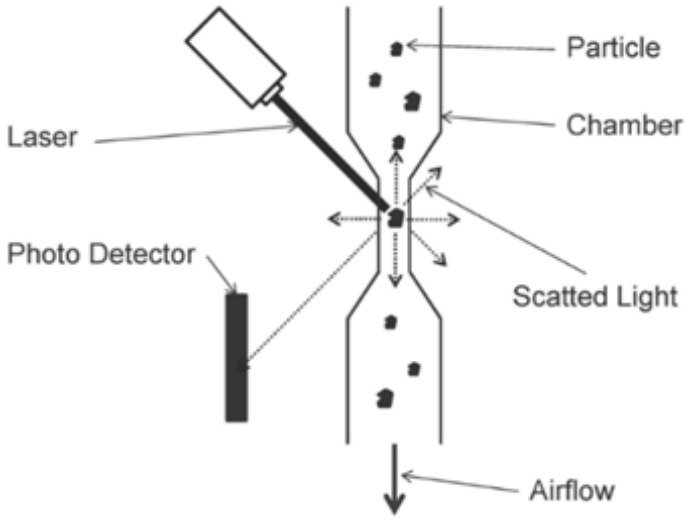

Figure 3. Basic light scattering system for counting particles in the air (Yi *et al*., 2015).

The Aerocet 831 was determined to be representative of these types of instruments and was selected for use in this study.

Objective

Determination of PM10 concentration with an FRM or FEM sampler requires expensive equipment, laboratory facilities, and the process of data collection is slow and tedious. EPA has promoted the notion of the "citizen scientist" where interested persons might set out to monitor environmental conditions. In these cases, a more rapid, less

expensive measurement would be desired to determine if there is a potential risk to human health or exceedance of NAAQS. Handheld particle counters, such as the Aerocet 831, have been considered for this purpose. However, the environments typical in agriculture do not have the ambient characteristics given in the specifications. Specifically, ambient airspeed can exceed 2 km/h. Therefore, the goal of this study was to determine the applicability of a handheld particle counter for estimating PM in an ambient environment over a broader range of airspeeds. In order to achieve this goal, the following objectives were studied:

1) Following the EPA protocol, determine the PM10 sampling effectiveness of the Aerocet 831 at 2, 8 and 24 km/h for monitoring monodisperse fluorescein particles of 3, 5, 7, 9, 10, 11, 13, 15 and 17 µm.
2) Determine the TSP sampling effectiveness of the Aerocet 831 at 2 and 8 km/h for monitoring monodisperse fluorescein particles of 3, 5, 7, 9, 10, 11, 13, 15 and 17 µm.
3) Evaluate the applicability of the Aerocet 831 for monitoring TSP and PM10 in typical agricultural environments.

CHAPTER II

EQUIPMENT AND PROCEDURES

Equipment

Wind Tunnel

Samplers used to collect PM10 are subjected to wind tunnel tests before they can be approved as part of a designated reference or equivalent method. The wind tunnel used for this study was originally fabricated in 1980 (McFarland and Ortiz 1982, 1984) to evaluate the performance of PM10 air sampler. The TAMU wind tunnel used in this study was located at the Center for Agricultural Air Quality Engineering and Science (CAAQES) at Texas A&M University. It consists of three sections, each section with 1.22 meters in length and 0.61m x 0.61m square cross section, a flared inlet, a sterman disk to uniform the generated particles, a flow straightener device to provide laminar flow, and a high efficiency particulate arresting HEPA filter for capturing the test particles before leaving the wind tunnel to prevent air contamination (Faulkner *et al.*, 2014) (Figure 4). The curved panels placed at the roof and the base of the test section were designed to reduce the pressure and achieve as high wind speed as 24 km/h. The Variable Frequency Drive of the fan installed at the end of wind tunnel was set at 8.65, 23.35 and 59 Hz to produce wind speed of 2, 8 and 24 km/h, respectively.

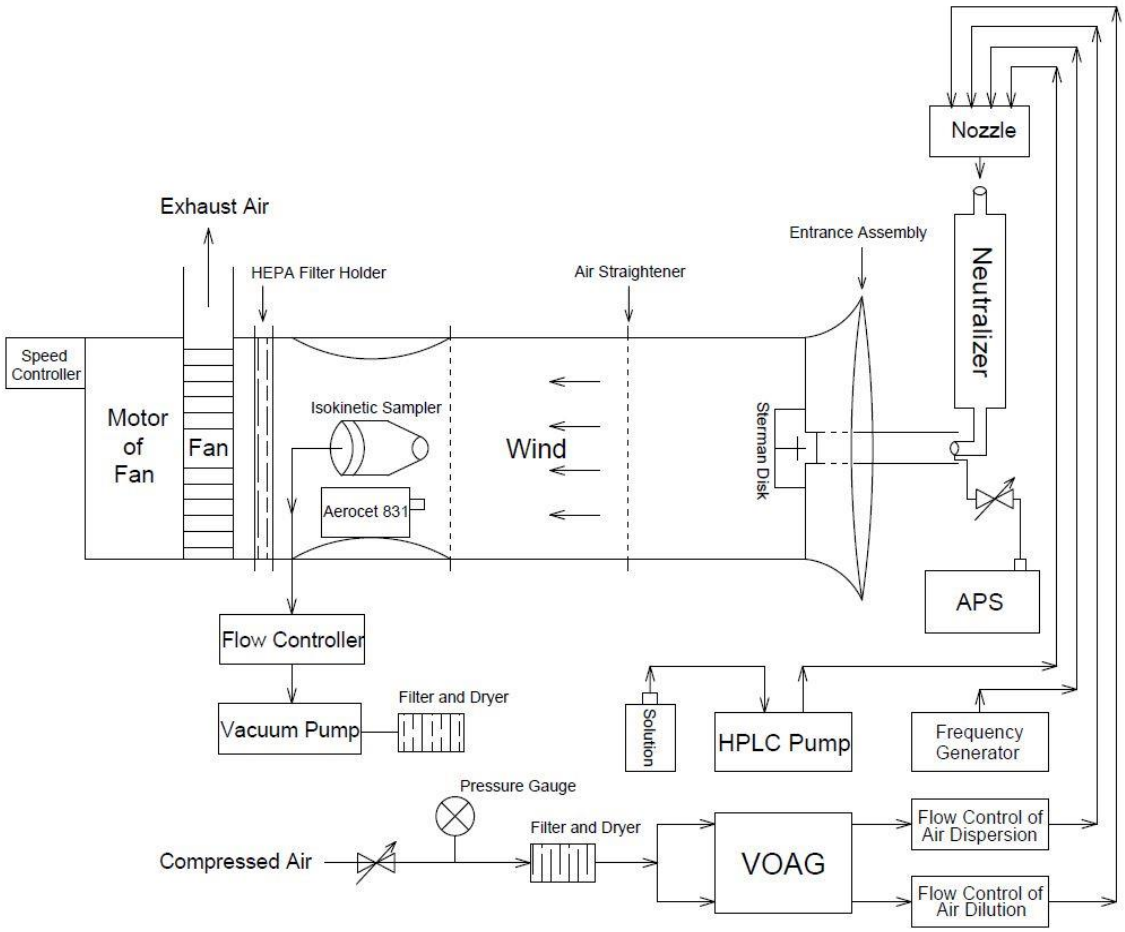

Figure 4. Schematic of TAMU wind tunnel, VOAG system and sampling system.

The performance of the wind tunnel, as required in the 40 CFR 53.42, must meet the criteria of wind speed uniformity and particle size precision shown in Table 1. To fully evaluate a PM10 sampler, the wind tunnel tests were required in 40 CFR 53.42 to evaluate the sampling effectiveness of candidate PM10 sampler at 2, 8 and 24 km/h for monodisperse aerosols of size 3, 5, 7, 9, 11, 13, 15, 20, 25 μm (size precision ± 0.5 μm).

Table 1. Performance requirement of wind tunnel for PM10 sampler (40 CFR 53.42).

Parameter	Performance requirement
Wind Speed	Mean wind Speed be within 10% for 2, 8, and 24 km/h
	Flow measurement precision be within ±2%
Particle Size	Geometric standard deviation for each size ≤ 1.1 (Coefficient of Variation≤ 10%)
	Candidate sampler blocks ≤ 15% of test section
	Proportion of multiplets ≤ 10%
	Verification techniques precision = 0.5 µm or 10% or better
	Sampling zone: horizontal dimension > 1.2 times the width of the test sampler at its inlet opening vertical dimension > 25 cm

Although it is specified mostly liquid particles, but particles in liquid form are not as uniform or stable as solid particles. In order to achieve the properties of particle similar to particles in ambient environment, the proposed tests will utilize only solid particles. Since the sampling effectiveness for 10 µm is a critical value for evaluating a PM10 sampler, the wind tunnel test on 10 µm is added, while the 20 and 25 µm is not included here since both PM10 and TSP sampling effectiveness of the Aerocet 831 for 17 µm reached close to 0%, and the aerodynamic particle sizer used in this test has maximum size detection of 20 µm.

Wind Velocity Uniformity

The velocity uniformity test on the TAMU wind tunnel was done in Faulkner et al. (2014). The wind velocity was measured in the wind tunnel across 33 measurement

points (Figure 5), which include 11 points spaced in 0.051 m intervals at three heights (76.2, 203.2, and 330.2 mm above the raised base) in the sampling plane. An anemometer (VelociCalc 8386, TSI, Inc., Shoreview, MN, USA) with accuracy of the greater of ± 3.0% or ± 0.015 m/s was used to sample at each point for 15 seconds at a rate of 1 Hz, and after 15 seconds the measurements were averaged and recorded. Each point was measured repeatedly at least 11 times. The results for all three wind speeds shown in Table 2 were proven to have met the mean wind speed and flow measurement precision requirements mentioned in table 1 (40 CFR 53.42).

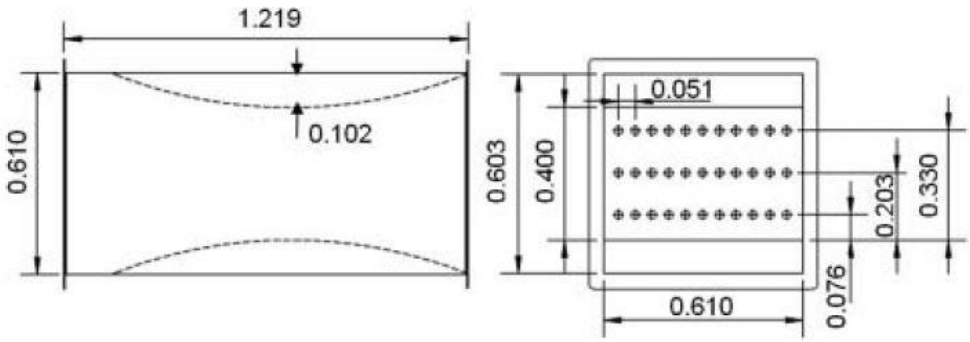

Figure 5. Position of 33 sampling points for wind velocity measurement (Faulkner *et al*., 2014).

Table 2. Wind velocity uniformity test results (Faulkner *et al*., 2014).

Nominal Wind Speed, km/h	Mean Wind Speed, km/h	COV, %	Maximum standard deviation
2	2.05	2.29	3.96
8	8.05	1.32	1.79
24	24.2	0.47	0.74

Particle Size Measurement

Particles of a certain size were generated from a prepared particle solution, but the actual particle size and distribution need to be verified after generation. The generated particles were introduced into an Aerodynamic Particle Sizer (APS, Model 3321, TSI, Inc., Shoreview, MN, USA) to monitor the mass frequency distribution of particles and check if the particles were monodispersed. For liquid particles, after entering the APS, the particle acceleration process through APS could cause the stretching of the particles and result in biased size measurement. In this case, liquid particles were impacted on coated slides and observed under microscope, and then a flattening coefficient was applied to calculate the spherical diameter of liquid particle (Faulkner and Haglund 2012). However for solid particles, the APS measurement process hardly had effect on the physical properties of the particles, thus the size of solid particles were assumed constant before and after entering the APS. Since only solid particles were produced and tested during this study, the particle size measurements were only dependent on the results reported form the APS, and generated particles were considered acceptable if the mass percentage of multiplets obtained from APS was less than 10%.

Vibrating Orifice Aerosol Generator

Monodisperse particles were generated from liquid particle solution using a vibrating orifice aerosol generator (VOAG; model 3450, TSI, Inc., Shoreview, MN,

USA). The liquid solution was constructed for each particle size with the combination of calculated mass of fluorescein ($C_{20}H_{12}O_5$, 90% purity, CAS 2321-07-5, Alfa Aesar, Heysham, Great Britain) and volume of ammonium hydroxide (NH_4OH) diluted in distilled water, and the calculations were listed in Equation (1) to (5) (Berglund and Liu, 1973).

$$Dp_a = Dp_p \sqrt{\frac{\rho_p}{\rho_w}} \tag{1}$$

Where Dp_a = aerodynamic particle diameter (μm), Dp_p = physical particle diameter (μm), ρ_w = water density (= 1 g/cm^3) and ρ_p = particle density (= 1.35 g/cm^3).

$$Dp_p = \left(\frac{6 * Q * C}{\pi * f}\right)^{1/3} \tag{2}$$

Where Q = solution flow rate (ml/s), C = volumetric concentration of aerosol material in the solution (dimensionless), and f = VOAG frequency (Hz).

$$C = \frac{m_f}{(\rho_f)(V)} \tag{3}$$

Where C= volumetric concentration of solid aerosol material (dimensionless), m_f = mass of fluorescein (g), ρ_f = density of fluorescein (g/cm^3), and V = final volume of solution, including unreacted ammonium hydroxide and DI water (mL) (ammonium hydroxide was added excessively to ensure complete reaction).

In order to form the product ammonium fluorescein ($C_{20}H_{15}NO_5$), the chemical reaction between fluorescein and ammonium hydroxide involved a replacement of an ammonium cation (NH^{4+}) for a hydrogen anion (H^+).

$$\rho_f = \rho_{af} * \left(\frac{M.W._f}{M.W._{af}}\right) \tag{4}$$

$$V_{NH_4OH} = \frac{m_f * F}{M.W._f * C_{NH_4OH}} \tag{5}$$

Where ρ_{af} = density of ammonium fluorescein (1.35 g/cm^3), $M.W._f$ = molecular weight of fluorescein (332.31 g/cm^3), $M.W._{af}$ = molecular weight of ammonium fluorescein (349.31 g/cm^3), V_{NH_4OH} = required volume of concentrated ammonium hydroxide (mL), C_{NH_4OH} = molar concentration of ammonium hydroxide (0.0145 mol/L), and F = desired excess factor (= 3.0).

A HPLC pump (Series 1500, ChromTech, Inc., Apple Valley, MN, USA) was used to pump the liquid solution at a flow rate of Q = 0.225 mL/min (Q = 0.0930 mL/min for 3 µm particle solution) into the VOAG nozzle head, where the liquid was then broken into many droplets of equal size by a vibrating orifice controlled by a frequency generator (frequency f = 150 kHz for 3 µm particle solution and f = 57 kHz for > 3 µm particle solution, adjust as needed to minimize multiplets). After the air dispersion and air dilution were adjusted properly, the compressed dry air were mixed with these droplets to form monodisperse, spherical solid particles, which were then introduced into wind tunnel after passing through the Kr-85 aerosol neutralizer (model

3054, TSI, Inc., Shoreview, MN, USA) to eliminate electrostatic charges between particles.

Obtained from the calculations (1)-(5), solution flow rate and VOAG frequency, the resulting composition of particle solutions of aerodynamic diameters 3, 5, 7, 9, 10, 11, 13, 15, 17 μm are shown in table 3.

Table 3. The composition of solid ammonium fluorescein particle solutions of aerodynamic diameters 3, 5, 7, 9, 10, 11, 13, 15, 17 μm.

Aerodynamic Particle Diameter, μm	**3**	**5**	**7**	**9**	**10**	**11**	**13**	**15**	**17**
Fluorescein Mass, g	0.172	0.801	2.203	4.687	6.433	8.565	14.146	21.740	31.657
NH_4OH Volume, mL	0.11	0.5	1.37	2.92	4.01	5.33	8.81	13.54	19.71

Isokinetic Air Sampler

The isokinetic air sampler installed with a 90 mm glass fiber filter (VWR International, LLC., Radnor, PA, USA) was used as the reference sampler to determine the sampling effectiveness of the Aerocet 831. The isokinetic air sampler captures particles without disturbing their paths by connecting to a vacuum pump, which was drawing the air through the isokinetic sampler at a standardized flow rate calculated by

equation (6) to maintain the velocity of the air going into the isokinetic nozzle equal to the average velocity of the undisturbed air in the wind tunnel. A HI-Q flow meter (D-AFC-09, Environmental Products, Inc., Vancouver, Canada) was used to adjust the air flow going through the isokinetic air sampler based on equation (6).

$$Q_s = \frac{44.1375 * P_a}{T} \quad (6)$$

Where Q_s = actual flow rate of air going through isokinetic sampler (L/min), P_a = ambient pressure (mmHg) and T = ambient temperature (K).

The nozzle sizes of isokinetic air sampler for wind speed of 2, 8, and 24 km/h are 2.6, 1.3 and 0.75 inches, respectively (Figure 6). The isokinetic air sampler and the Aerocet 831 were co-located in the wind tunnel to collect and monitor particles simultaneously (Figure 7).

Figure 6. Three different nozzles of isokinetic air sampler.

Figure 7. Location of isokinetic air sampler and Aerocet 841 inside wind tunnel.

Fluorometer

The weight measurement of fluorescein solid particles removed by the filter of isokinetic air sampler was based on their fluorescence intensity unit (FIU) measured by a Fluorometer (Model No. FM109515, Barnstead/Thermolyne Corp., Dubuque, IA, USA). Each Fluorochrome has its own unique spectra for excitation and emission, which show relative fluorescence Intensity and can be measure by a monochromator over a series of wavelengths. The maximum excitation and emission wavelength for fluorescein are 495 nm and 519 nm, respectively (Dawe *et al.* 2006). Light directed through a narrow band pass filter in this fluorometer has wavelength range of 340-650 nm

(Barnstead/Thermolyne Corp., 1999). With the primary excitation filter of NB490 and the secondary emission filter of SC515, the fluorometer will detect emission light only at a wavelength of 515 nm, resulting in a measurement of the FIU of the fluorescein particles. Afonso *et al*. (1999) found a positive relation between the mass of liquid particles of uranine fluorescein and its FIU at low concentration range of 0.006-20 μg/ml (corresponding to concentrations of 6.25 x 10^{-5}% to 0.002% in g/ml). However, no mathematical correlation was found between the FIU and mass of solid fluorescein particles, which exceeded 20 μg. The fluorometer used in this study was tested to demonstrate the validity of this positive relationship with high range of fluorescein mass (explained in the section of Correlation between Fluorescein mass and FIU).

Procedures

Solid Ammonium Fluorescein Particle Generation

In order to create a solution at a specific particle size, a known mass of fluorescein measured by an analytical balance (Mettler Toledo analytical balance, Columbus, OH, USA), and a known volume of 14.5N NH_4OH measured by a micropipette (Eppendorf AG., Hamburg, Germany), were mixed in a fume hood. The resulting volume of the solution was adjusted to 1000 mL by distilled water. A sonicating system was used to completely solubilize solid particles. Nine solutions were made for particle sizes 3, 5, 7, 9, 10, 11, 13, 15 and 17 μm (Table 3) and kept in their

amber glass containers at room temperature. For each test, the prepared solution was connected to the HPLC pump and transferred to the nozzle of VOAG at the constant flow rate after the system was primed with pure ethanol. The frequency of the vibrating orifice was maintained by the frequency generator to break solution into droplets. Compressed air was directed into VOAG and the flow rate and air distribution were observed and controlled before the air was let into the nozzle and mixed with fluorescein droplets.

Once a straight streamline under the nozzle was observed, the discharge of generated particles from the nozzle was conducted to a neutralizer. Prior to introduction into the wind tunnel, the generated particles were directed into the APS to verify the particle size. If the mass distribution obtained from APS did not show a monodisperse histogram, the frequency of vibrating orifice, air dilution, and distribution were adjusted sequentially until the mass percentage of multiplets and satellites was less than 10%. The finalized frequency was recorded and used to calculate the aerodynamic diameter of the resulting particles by equation (1). Table 4 shows the finalized VOAG frequency values used in this study to produce particles of nominal sizes 3, 5, 7, 9, 10, 11, 13, 15, 17 μm, and their calculated aerodynamic diameter and APS volume mean diameter. The particle mass distribution recorded by the APS for each generated nominal particle size is shown in Appendix A.

Table 4. The VOAG frequency adjusted to produce particles of nominal sizes 3, 5, 7, 9, 10, 11, 13, 15, 17 µm, and their corresponding APS volume mean diameter and calculated aerodynamic diameter.

Nominal Diameter, µm	**VOAG Frequency, KHz**	**APS Volume Mean Diameter $D_{APS,VMD}$, µm**	**Calculated Diameter D_a, µm**
3	132.23	3.0	3.11
5	56.910	5.04	4.97
5	60.290	4.99	4.88
7	49.076	6.83	7.33
7	54.163	7.16	7.10
9	55.748	8.8	9.04
10	58.830	10.3	9.87
10	60.027	9.88	9.79
11	57.270	11.3	10.83
13	55.950	14.9	13.05
13	58.629	13.7	12.84
15	55.790	14.5	15.07
15	58.269	15.9	14.81
17	54.242	18.1	17.24

Correlation between Fluorescein Mass and FIU

The generated solid ammonium fluorescein particles of 5 µm was discharged from the neutralizer directly to the isokinetic sampler outside of the wind tunnel. The isokinetic sampler therefore captured all particles without loss on its glass fiber filter. The collecting process was timed and each three replicate samples were collected at

different sampling durations in order to obtain different fluorescein mass. The sampling durations are listed in table 5.

Table 5. Different fluorescein mass collected from 5 μm fluorescein solution and their corresponding FIU values.

Operation Duration, s	Fluorescein Mass, μg	FIU per mL Solution
3	9	82
10	30	209
25	75	361
40	120	500
60	181	828
90	271	1170
120	361	1441
180	542	1757
240	723	2063
300	903	2386
360	1084	2546
420	1265	2442
480	1445	2706
540	1626	2468

After each test, the filter was transferred to a container and the remaining particles adhered to the inner surface of the isokinetic sampler nozzle were washed with a 0.01N NH_4OH solution directly into the container. The total volume of NH_4OH solution added to the container was controlled to approximately 40 mL to dissolve fluorescein solid particles. The actual volume of NH_4OH added was obtained by

weighing the filter container with an analytical balance (Model MS303S, Mettler Toledo, Switzerland) before and after NH_4OH was added. The resulting solutions were stored in closed containers at room temperature for at least 12 hours, and then 10 mL of each solution was transferred to a fluorometer test tube to measure its FIU (Table 5). The fluorescein mass was calculated based on equation (7).

$$m_f = Q * \frac{t}{60} * C * \rho_f * 10^6 \quad (7)$$

Where m_f = mass of fluorescein (ug), Q = solution flow rate (mL/min), t = operation time (s), C= volumetric concentration of solid aerosol material (dimensionless), ρ_f = density of fluorescein (g/cm^3), $C * \rho_f$ = mass of fluorescein added to prepare the particle solution.

The FIU values were plotted as a function of fluorescein mass in Microsoft Excel® and a non-linear (Gauss error) model was fitted to the data points by adjusting coefficients shown in Equation (8 & 9) (i.e. 5084.6 and 685.9) to minimize the SSE (sum of squared errors) between data points and fitted model (Figure 8).

$$FIU = \frac{5084.6}{\sqrt{\pi}} * \int_0^{\frac{m_f}{685.9}} \exp(-u^2)\, du \quad (8)$$

Or,

$$m_f = 685.9 * erfinv\left(\frac{FIU}{2542.3}\right) \quad (9)$$

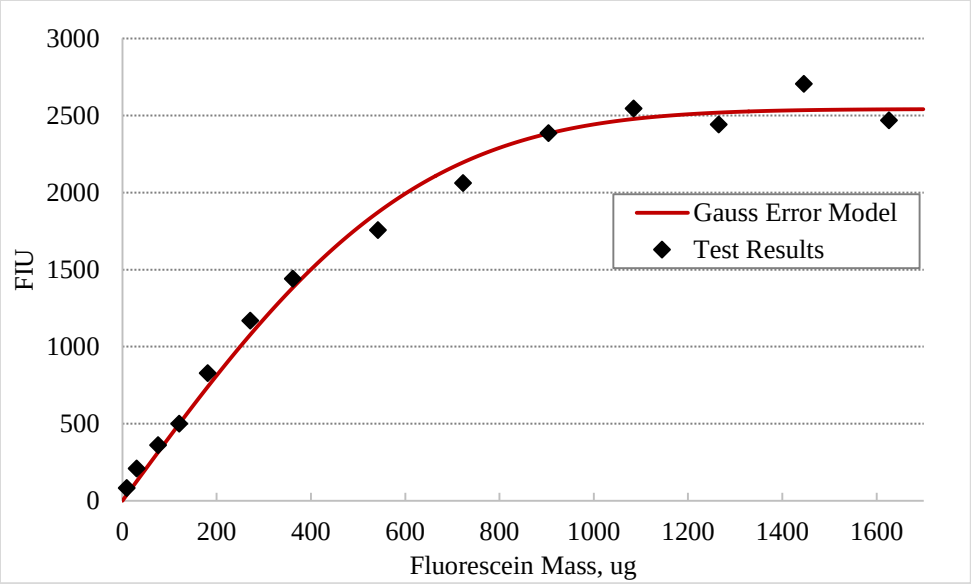

Figure 8. Plot of FIU as a function of fluorescein mass for 5µm fluorescein particle.

This Gauss Error model fit well with the data points and covered a wide range of fluorescein mass from 9 to 1626 µg. For this study, the range from 0 to 240 µg was used to convert measured FIU of fluorescein particle to its fluorescein mass.

Aerosol Sampling

Generated fluorescein solid particles of size 3, 5, 7, 9, 10, 11, 13, 15 and 17 µm were introduced sequentially into the wind tunnel, which was operated at wind speeds of 2, 8, and 24 km/h. The Variable Frequency Drive installed at the end of the wind tunnel fan was adjusted to achieve the desired wind speed (specified in the Wind Tunnel section). The isokinetic air sampler was loaded with a 90 mm glass fiber filter and then located at the center of the curved section of the wind tunnel. The Aerocet 831 was co-

located parallel to the isokinetic air sampler to monitor and collect fluorescein particles simultaneously. The vacuum pump connected to the isokinetic air sampler was adjusted to a constant standardized flow rate. The duration of each test was 15 minutes sampling time and was repeated at least three times or until a coefficient of variance (COV) less than 10% was obtained. The TSP and PM10 mass concentrations ($\mu g/m^3$) were recorded by the Aerocet 831 once per minute over the test duration. The data were downloaded using the Met-One software to a personal computer after the set of the three tests was completed. The filter was removed from the isokinetic air sampler after each test and placed into a container with 0.01N NH_4OH solution for FIU measurement. The VOAG system was flushed with pure ethanol to remove any remaining fluorescein solution from the system. The mass concentration of particles deposited on the isokinetic air sampler filter was determined by equation (10).

$$C_{iso} = \frac{m_f * 10^3}{Q_s * t} \tag{10}$$

Where m_f = mass of fluorescein (µg) (calculated from equation 10), Q_s = actual flow rate of air going through isokinetic sampler (L/min) (calculated from equation 6), t = sampling time, 15 min.

CHAPTER IV

RESULTS, DISCUSSION AND CONCLUSION

Sampling Effectiveness of Aerocet 831

The observed sampling effectiveness η_i for each particle size i was determined by the ratio of PM mass concentration monitored by the Aerocet 831, C_{Aer} (µg/m^3), to the mass concentration of particles collected by the isokinetic air sampler, C_{iso} (µg/m^3), (Equation 11).

$$\eta_i = \frac{C_{Aer}}{C_{iso}} \tag{11}$$

The coefficient of variation (COV) of the sampling effectiveness for each size was calculate by dividing the standard deviation, σ, of the sampling effectiveness for the total n = 3 replicates by the average sampling effectiveness $\bar{\eta}$ (Equation 12 & 13).

$$\sigma = \sqrt{\frac{\sum_{i=1}^{n} \eta_i^2 - \frac{1}{n}(\sum_{i=1}^{n} \eta_i)^2}{n-1}} \tag{12}$$

$$COV = \frac{\sigma}{\bar{\eta}} \times 100\% \tag{13}$$

Table 6 shows the observed sampling effectiveness values of Aerocet 831 for sampling particles of nominal size 3, 5, 7, 9, 10, 11, 13, 15, and 17 µm at wind speed of 2, 8 and 24 km/h, and their corresponding COV values. The corrected sampling effectiveness values in Table 6 are directly related with curve fitting, therefore will be discussed in the next (Curve Fitting and Mutiplet Correction) section.

Table 6. Sampling effectiveness results of Aerocet 831 at 2, 8 and 24 km/h.

		Wind Speed at 2 km/h				Wind Speed at 8 km/h				Wind Speed at 24 km/h			
	Nominal Size (µm)	Calculated size[b] (µm)	Sampling Effectiveness, %		COV, %	Calculated size (µm)	Sampling Effectiveness, %		COV, %	Calculated size (µm)	Sampling Effectiveness, %		COV, %
			Observed	Corrected[c]			Observed	Corrected			Observed	Corrected	
PM10	3	3.11	101.57	100.00	9.15	3.11	112.57	100.00	1.35	3.11	140.88	100.00	8.24
	5	4.97	100.97	96.76	3.52	4.88	122.28	99.05	4.06	4.88	113.09	99.89	4.38
	7	7.33	97.19	79.64	9.39	7.10	111.25	87.91	9.43	7.10	122.76	99.83	3.17
	9	9.04	13.14	24.06	9.04	9.04	36.58	49.96	17.3[a]	9.04	92.02	96.25	7.16
	10	9.87	9.51	9.65	29.0[a]	9.79	28.52	34.44	9.03	9.87	104.35	86.21	6.53
	11	10.83	5.59	2.15	9.00	10.83	29.68	18.32	7.65	10.83	80.99	74.67	12.2[a]
	13	13.05	6.45	0.01	9.29	12.84	14.29	4.29	17.9[a]	12.84	23.45	30.65	9.19
	15	15.07	4.26	0.06	10.3[a]	14.81	11.21	0.89	0.57	14.81	15.28	7.50	11.0[a]
	17	17.24	4.23	0.00	9.69	17.24	5.98	0.07	9.85	17.24	5.97	0.62	9.49
TSP	3	3.11	121.31	99.99	8.86	3.11	115.47	100.00	9.26				
	5	4.97	125.60	97.20	5.75	4.88	137.27	99.97	18.5[a]				
	7	7.10	120.49	93.93	7.69	7.10	112.41	99.95	6.94				
	9	9.04	71.12	80.72	5.99	9.04	87.81	98.81	3.93				
	10	9.87	72.18	72.10	9.38	9.79	103.38	97.46	9.41				
	11	10.83	60.83	63.77	7.44	10.83	99.58	92.86	8.82				
	13	13.05	44.12	17.55	9.21	13.05	73.95	71.33	6.24				
	15	15.07	30.68	27.30	7.07	15.07	45.79	44.41	6.76				
	17	17.24	18.65	16.40	6.45	17.24	15.15	17.37	9.01				

[a] COV exceeds 10%.
[b] Particle size calculated using Equation (1).
[c] Corrected sampling effectiveness for multiplets and satellites.

For the observed PM10 readings, the sampling effectiveness values for particles of nominal size 3, 5 and 7 µm at 8 and 24 km/h exceeded 100%. The cause of these results could arise from one of the following five potential causes:

1) The operation principles of Aerocet 831 and isokinetic air sampler are different. The Aerocet 831 is counting and sizing particles using laser scattering, while the operation of isokinetic air sampler is based on filtration.
2) The pore size of the glass fiber filter used in isokinetic air sampler is 0.7 µm, while the minimum particle size Aerocet 831 can detect is 0.3 µm. Even though

the concentration of particles less than 0.7 μm in diameter shown in APS is very low, the Aerocet 831 can detect and count these particles. However, these small particles will pass through the filter of isokinetic air sampler and not be collected. According to a study done at Los Angeles Basin (Singh *et al*., 2002) to measure PM10 chemical compounds and their size distribution resulting from local emissions, the ambient fine particles of size 0.1-0.35 μm (condensation mode) and 0.35-1.0 μm (droplet mode) had respectively 14% and 24% nitrate compounds NH_4NO_3. Since the particle solutions made for the wind tunnel tests had 3 times excess volume of NH_4OH, therefore the aerosols produced from these solutions remained some NH_4^+, and they might interact with the nitrate in the air and formed very fine particles (< 0.7 μm).

3) The wind tunnel measurements on mineral dust aerosols of Alfaro et al. (1998) showed a statistically significant decrease of the Mass Median Diameter from 14.2 μm to 1.5 μm with the increase of wind speed from 1.26 km/h to 2.376 km/h. It is possible that the generated small aerosols (of nominal size 3, 5 and 7 μm) would break into even smaller aerosols (especially aerosols < 0.7 μm) in the wind tunnel due to such high wind speed as 8 and 24 km/h.
4) Aerocet 831 is designed to count and size particles, not weighing them. It is recommended in its operation manual (Met One Instruments, Inc., 2014) to apply a K-factor as the particle “standard” density on the reported data to obtain mass concentration. However, the APS measures directly the weight, size and number

of particles. This fact explains that the mass concentration reported by Aerocet 831 and APS are not similar.

5) The performance accuracy of Aerocet 831 is ± 10% based on its operation manual (Met One Instruments, Inc., 2014), and this could be the reason for the observed TSP sampling effectiveness of nominal 3, 5 and 7 μm particles exceeding 100% at 2km/h. Because of the ± 10% variation in the Aerocet 831 reading numbers, some COVs of PM10 and TSP observed sampling effectiveness data in Table 6 exceed 10% (40 CFR 53.43(a)(2)(ix)).

6) It is possible that the orientation of the Aerocet 831 relative to the wind direction inside the wind tunnel has some effects on its performance. The Aerocet 831 operates with a flow rate of 2.83 L/min. When the wind speed inside the wind tunnel increases to more than 2 km/h, and the Aerocet 831 is facing parallel to the wind, the speed of particles travel into the Aerocet 831 is higher than the speed the Aerocet 831 draws particles. Thus, the particles would be accumulating at the inlet of the Aerocet 831 and forcing themselves to enter into the device, resulting in particle breaking. In contrast, when Aerocet 831 is placed perpendicular to the wind direction, the particles would travel in the direction of the resultant of the two perpendicular wind speed vectors, thus they are likely to hit the side of the Aerocet 831 inlet and no be detected.

Curve Fitting and Mutiplet Correction

At each wind speed of 2, 8 and 24 km/h, the observed sampling effectiveness data were plotted as a function of particle size in Microsoft Excel® (Figure 10 & 11 Test Data). A lognormal distribution curve was fitted to these data points by adjusting the cut-point α and slope β in equation 14 to minimize the SSE between the observed and predicted effectiveness.

$$\eta(d_p) = 1 - \frac{1}{ln(\beta)\sqrt{2\pi}} exp\left[-\frac{1}{2}\left(\frac{ln(d_p) - ln(\alpha)}{ln(\beta)}\right)^2\right] \quad (14)$$

Particle mass frequency distribution (Appendix A) collected with the APS for each particle size at each wind speed was then applied to its corresponding observed sampling effectiveness for satellites and multiplets correction (Haglund *et al*., 2002). Before the satellites and multiplets correction, the correction factor f was calculated for each size of particles generated, and applied to correct all particle sizes in the APS particle mass frequency distribution.

$$f = \frac{D_a}{D_{APS,VMD}} \quad (15)$$

Where D_a = calculated aerodynamic diameter, $D_{APS,VMD}$ = volume mean diameter reported by the APS, values of D_a and $D_{APS,VMD}$ in this study are shown in Table 4.

The corrected sampling effectiveness value (shown in Table 6) was obtained as a product of APS relative mass frequency distribution of each particle size and the observed sampling effectiveness curve at each wind speed (Equation 16) (Figure 9).

$$E_i = \int [\eta(d_p) \cdot f_{m,i}(d_p)] dd_p \tag{16}$$

Where E_i = corrected sampling effectiveness for test particle i, η = modeled observed sampling effectiveness for various particle size, $f_{m,i}$ = APS reported relative mass frequency distribution of test particle i.

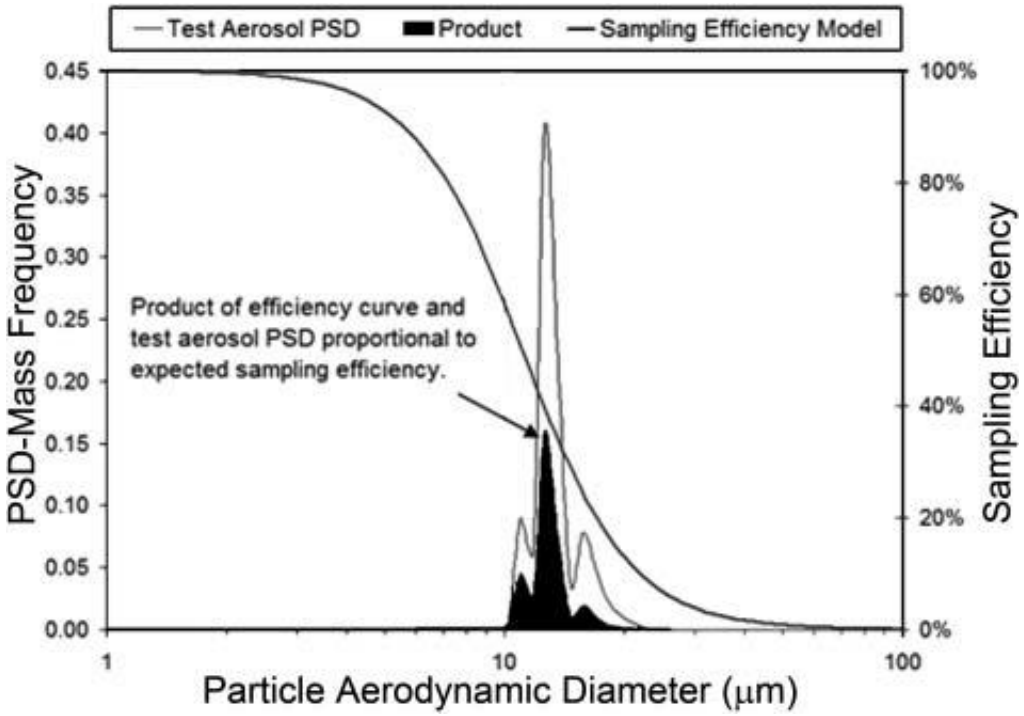

Figure 9. Calculation example of the corrected sampling efficiency for generated test aerosols with multiplets and satellites (Faulkner *et al*., 2014).

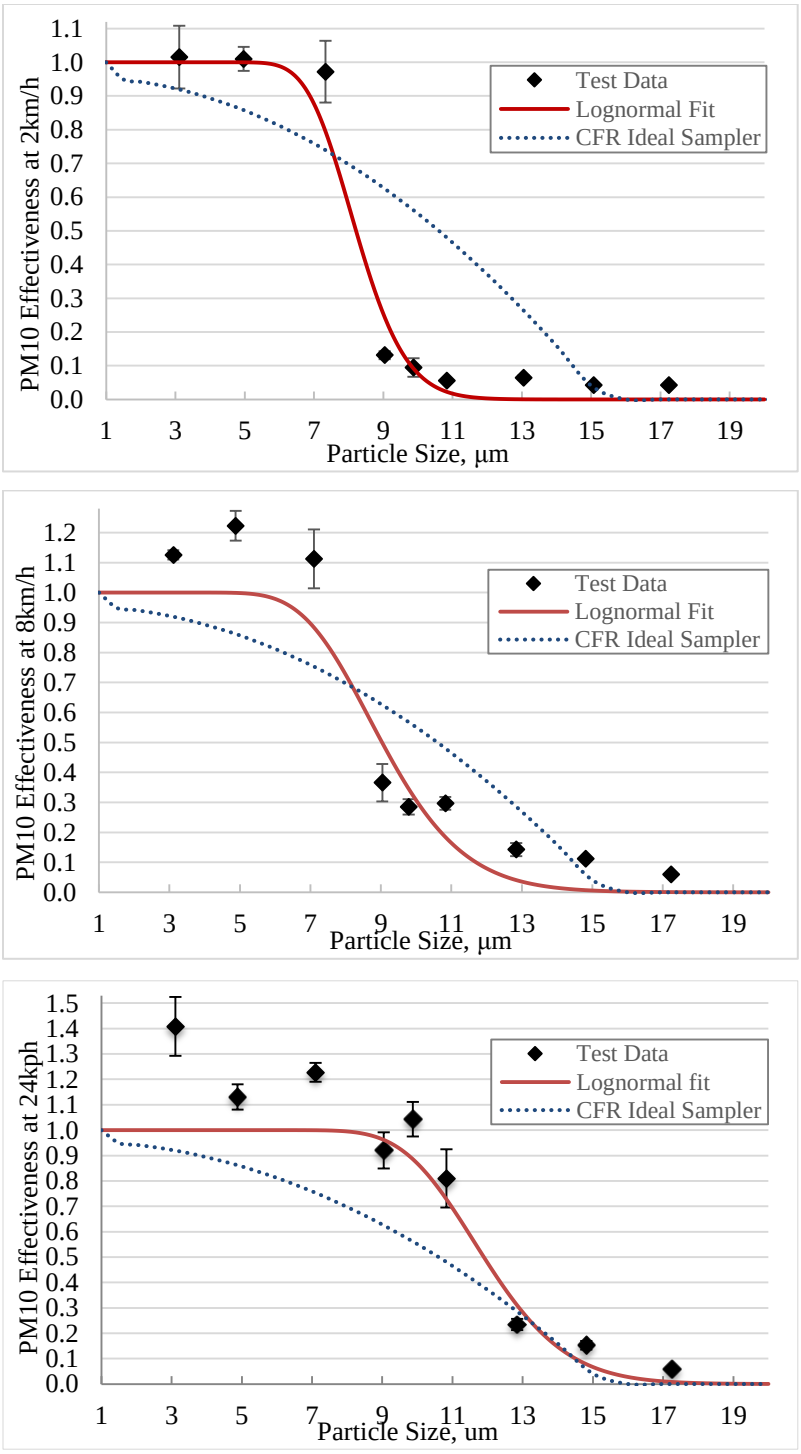

Figure 10. PM10 sampling effectiveness curves with multiplet correction at wind speed of 2, 8 and 24 km/h.

The obtained values were fitted again to lognormal distribution curves (shown in Figure 10 &11 Lognormal Fit) based on equation 14 using the above-mentioned method. The effectiveness curve for ideal PM10 sampler was added to Figure 10 &11 for comparison.

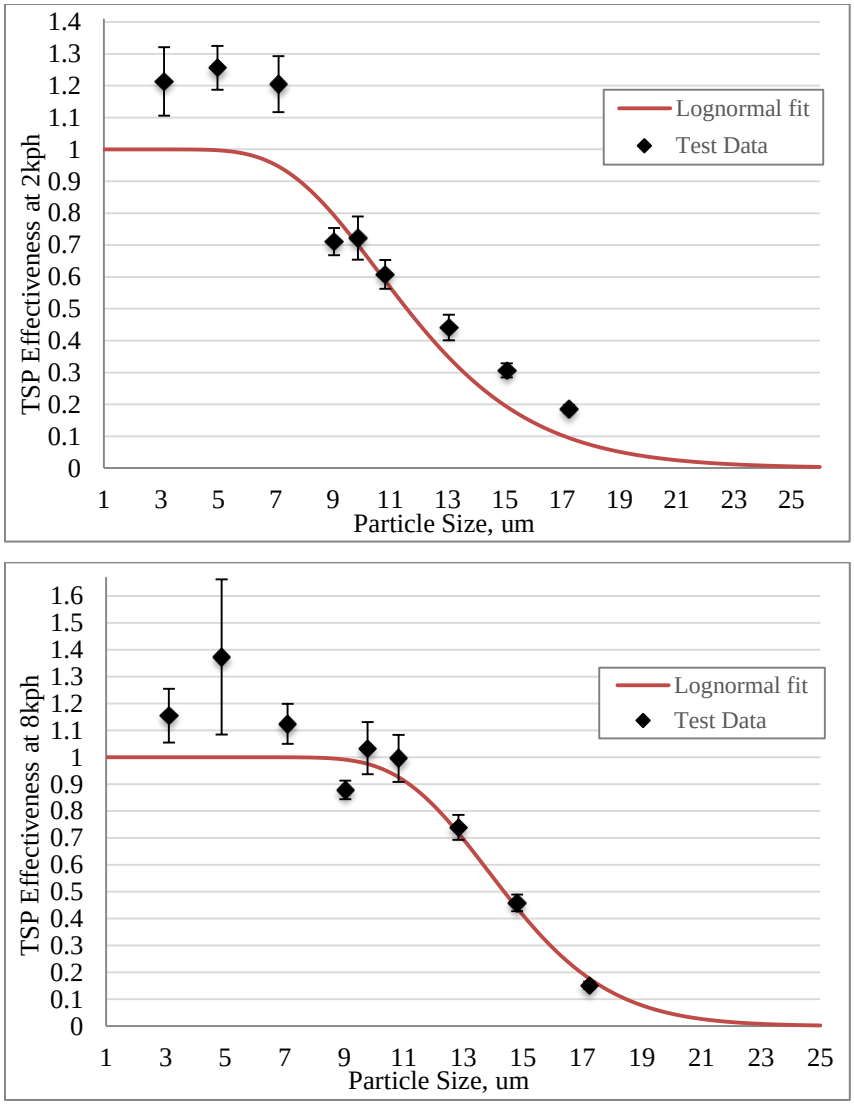

Figure 11. TSP sampling effectiveness curves with multiplet correction at wind speed of 2 and 8 km/h.

The resulting cut-point and slope for each fitted corrected sampling effectiveness curve were shown in Table 7.

Table 7. Cut-point and slope of lognormal corrected sampling effectiveness curves at 2, 8 and 24 km/h.

	PM10 Effectiveness Curve			**TSP Effectiveness Curve**	
	2kph	**8kph**	**24kph**	**2kph**	**8kph**
50% Cut Point, µm	8.21	9.03	11.89	11.58	14.37
Slope	1.15	1.22	1.17	1.35	1.22

From Figure 10 and Table 7, the cut-points for PM10 effectiveness curves at wind speed of 2, 8 and 24 km/h were respectively 8.21, 9.03 and 11.89 µm. In addition, all slope of their curves are steeper than the ideal PM10 curve's, which shows an advantage of the Aerocet 831 over ideal PM10 sampler, since steeper slope means collecting more smaller particles and excluding more larger particles. From the PM10 effectiveness curve at 2 km/h, the test data fits very well with the lognormal distribution curve, and the slope of the curve is almost close to 1.0, which suggests that the Aerocet 831 has a good performance at 2 km/h. From the PM10 effectiveness curve at 8 and 24 km/h, there are noticeable oversampling at small particles of size 3, 5 and 7 µm, and their cut-points are not in the range of 10 ± 0.5 µm, therefore the Aerocet 831 is not recommended to be used under such high wind speed as 8 and 24 km/h.

From Figure 11 and Table 7, the cut-points for TSP effectiveness curves at wind speed of 2 and 8 km/h were respectively 11.58 and 14.37 µm. It is indicated that there are oversampling at small particle sizes 3, 5 and 7 µm, and the effectiveness starts to decrease from particle size of 9 and 11 µm respectively for wind speed of 8 and 24 km/h. It is desired for a TSP sampler to collect particles of sizes up to 50 µm, but the maximum size detection of Aerocet 831 shown from the figure 11 is only about 23 µm. Thus, it is not recommended to use the Aerocet 831 for measuring TSP at different wind speeds.

Each of the PM10 effectiveness curve was numerically integrated with an idealized ambient particle size distribution provided in 40 CFR 53.43 Table D-3 (Appendix B, C and D) to calculate the expected mass concentrations of Aerocet 831 (Table 8).

Table 8. Expected mass concentration of Aerocet 831 based on its PM10 sampling performance at three wind speeds.

Wind Speed, km/h	**Expected mass concentration, µg/m^3**	**Percent Difference in Expected Mass Concentration between Aerocet 831 and Ideal PM10 Sampler, %**
2	125.326	12.9
8	135.874	5.57
24	166.784	15.9
Ideal PM10 Sampler	143.889	N/A

The expected mass concentration for Aerocet 831 at 2 and 8 km/h both fall within ± 15% of that predicted for the ideal sampler, but it slightly exceeds the 15% difference at 24 km/h for less than 1%.

Conclusion

The handheld particle monitor Aerocet 831 was tested in a wind tunnel at three different wind speeds to obtain its PM10 and TSP effectiveness for monitoring nine different size of monodisperse aerosols. Additional tests were performed to find out a mathematical correlation equation between FIU and a wide range of fluorescein particle mass (0-240 μg). The sampling effectiveness values were calculated, corrected and fitted to lognormal distribution curves.

From its PM10 sampling effectiveness, the Aerocet 831 is indicated having good performance for monitoring PM10 at wind speed of 2 km/h, due to the fact that its observed effectiveness data fits well with the lognormal distribution curve and the slope of the curve is very close to 1.0. However, its applicability for measuring PM10 at 8 and 24 km/h is limited due to the oversampling at small particle sizes.

From its TSP sampling effectiveness, the performance of Aerocet 831 for monitoring TSP is indicated not optimal at different wind speeds, since there are oversampling shown at small particle sizes and the maximum particle size detection is

only about 23 μm, while the expected detecting size range for a TSP sampler would be from 0 to 50 μm.

If the Aerocet 831 could be redesigned to fit a broader range of wind speeds, and the inaccuracy of Aerocet 831 could be minimized, the particles mass could be directly measured (similar to the APS system), the applicability of Aerocet 831 will be greatly improved. In many cases, the wind direction in a specific environment may be unknown or not consistent, therefore more research needs to be done to find out whether the orientation of Aerocet 831 relative to the wind direction has effect on its monitoring performance. Field research on Aerocet 831 is also needed to evaluate its performance for monitoring ambient particles in indoor agricultural facilities such as poultry house, where the wind speed is low. If Aerocet 831 is proved to have good performance in the field, the application of this device will become more popular, and it will also contribute to the future research in the air quality field (especially in particulate matter).

REFERENCES

Afonso, A. A., Monroy, D., Stern, M. E., Feuer, W. J., Tseng, S. C., & Pflugfelder, S. C., 1999. "Correlation of tear fluorescein clearance and Schirmer test scores with ocular irritation symptoms." *Ophthalmology*, 106(4), 803-810.

Alfaro, S. C., Gaudichet, A., Gomes, L., and Maillé, M., 1998. "Mineral aerosol production by wind erosion: aerosol particle sizes and binding energies." *Geophysical Research Letters*, 25(7), 991-994.

Barnstead/Thermolyne Corp., 1999. "Turner quantech digital filter fluorometer operation manual." LT1095X1. https://www.nbtc.cornell.edu/sites/default/files/Full%20TQ%20fluorometer%20manual.pdf

Berglund, R. N., & Liu, B. Y., 1973. "Generation of monodisperse aerosol standards." *Environmental Science & Technology*, 7(2), 147-153.

Buser, M. D., Parnell Jr, C. B., Shaw, B. W., and Lacey, R. E., 2007. "Particulate matter sampler errors due to the interaction of particle size and sampler performance characteristics: background and theory." *Trans. ASABE*, 50(1), 221-228.

Davidson, C. I., Phalen, R. F., and Solomon, P. A., 2005. "Airborne particulate matter and human health: A review." *Aerosol Science and Technology*, 39(8), 737-749.

Dawe, G. S., Schantz, J. T., Abramowitz, M., Davidson, M. W., and Hutmacher, D. W., 2006. "Light microscopy." *Tech. Microsc. Biomed. Appl*, Part B, 60.

Faulkner, W. B. and Haglund, J. S., 2012. "Flattening coefficients for oleic acid droplets on treated glass slides." *Aerosol Science and Technology*, 46(7), 828-832.

Faulkner, W. B., Smith, R., and Haglund, J., 2014. "Large particle penetration during PM10 sampling." *Aerosol Science and Technology*, 48(6), 676-687.

Haglund, J. S., Chandra, S., and McFarland, A. R., 2002. "Evaluation of a high volume aerosol concentrator." *Aerosol Science & Technology*, 36(6), 690-696.

International Standard Organization (ISO), 1995. "Air quality: particle size fraction definitions for health-related sampling." *ISO*, 7708:1995(E).

Lacey, R. E. and Faulkner, W. B., 2015. "Uncertainty associated with the gravimetric measurement of particulate matter concentration in ambient air." *Journal of the Air & Waste Management Association*, 65(7), 887-894.

McFarland, A. R., Ortiz, C. A., and Bertch Jr, R. W., 1984. "A 10 μm outpoint size selective inlet for hi-vol samplers." *Journal of the Air Pollution Control Association*, 34(5), 544-547.

McMurry, P., Shepherd, M., and Vickery, J., 2004. "Particulate matter science for policy makers; a NARSTO assessment." Cambridge University Press (New York).

Met One Instruments, Inc., 2014. "Aerocet 831 manual." 831-9800 Rev D1.doc. http://www.metone.com/docs/831_operationmanual.pdf.

Schwartz, J., 1994. "Air pollution and daily mortality: a review and meta analysis." *Environmental Research*, 64(1), 36-52.

Singh, M., Jaques, P. A., and Sioutas, C., 2002. "Size distribution and diurnal characteristics of particle-bound metals in source and receptor sites of the Los Angeles Basin." *Atmospheric Environment*, 36(10), 1675-1689.

United States Environmental Protection Agency (USEPA), 2017. "Procedures for testing performance characteristics of methods for PM10." 40 CFR Part 53, Subpart D.

Valavanidis, A., Fiotakis, K., and Vlachogianni, T., 2008. "Airborne particulate matter and human health: toxicological assessment and importance of size and composition of particles for oxidative damage and carcinogenic mechanisms." *Journal of Environmental Science and Health*, Part C, 26(4), 339-362.

Wanjura, J. D., Parnell Jr, C. B., Shaw, B. W., and Lacey, R. E., 2005. "Design and evaluation of a low-volume total suspended particulate sampler." *Transactions of the ASAE*, 48(4), 1547-1552.

Yi, W. Y., Lo, K. M., Mak, T., Leung, K. S., Leung, Y., and Meng, M. L., 2015. "A survey of wireless sensor network based air pollution monitoring systems." *Sensors*, 15(12), 31392-31427.

APPENDIX A

PARTICLE SIZE DISTRIBUTION

Table 9. Size distribution of particles of nominal sizes 3, 5, 7, 9, 10 µm generated from wind tunnel tests.

Nominal Particle Diameter, µm	**3**	**5**	**5**	**7**	**7**	**9**	**10**
Calculated Aerodynamic Diameter, µm	**3.11**	**4.97**	**4.88**	**7.33**	**7.10**	**9.04**	**9.87**
Size Distribution	**Mass Concentration, mg/m^3**						
1.715	0.00	0.00	0.00	0.00	0.00	0.00	0.00
1.843	0.00	0.00	0.00	0.00	0.00	0.00	0.00
1.981	0.01	0.00	0.00	0.00	0.00	0.00	0.00
2.129	0.02	0.00	0.00	0.00	0.00	0.00	0.00
2.288	0.11	0.00	0.00	0.00	0.00	0.00	0.00
2.458	0.72	0.00	0.00	0.00	0.00	0.00	0.00
2.642	6.07	0.00	0.00	0.00	0.00	0.00	0.00
2.839	17.30	0.00	0.00	0.00	0.00	0.00	0.00
3.051	6.87	0.00	0.00	0.00	0.00	0.00	0.00
3.278	2.67	0.00	0.01	0.00	0.00	0.00	0.00
3.523	4.52	0.02	0.01	0.00	0.00	0.00	0.00
3.786	2.21	0.07	0.13	0.00	0.00	0.00	0.00
4.068	1.19	0.33	0.42	0.00	0.00	0.00	0.00
4.371	0.46	1.07	1.29	0.00	0.00	0.00	0.00

Table 9. Continued.

Nominal Particle Diameter, µm	**3**	**5**	**5**	**7**	**7**	**9**	**10**
Calculated Aerodynamic Diameter, µm	**3.11**	**4.97**	**4.88**	**7.33**	**7.10**	**9.04**	**9.87**
Size Distribution	**Mass Concentration, mg/m^3**						
4.698	0.12	4.59	4.10	0.02	0.01	0.00	0.00
5.048	0.06	6.27	8.92	0.08	0.02	0.00	0.00
5.425	0.02	1.86	3.74	0.31	0.09	0.00	0.00
5.829	0.00	0.51	0.54	1.97	0.67	0.03	0.00
6.264	0.00	0.15	0.12	3.30	2.37	0.05	0.00
6.732	0.00	0.06	0.08	4.60	5.66	0.12	0.02
7.234	0.00	0.04	0.06	5.54	10.80	1.22	0.08
7.774	0.00	0.02	0.05	2.41	4.13	8.64	0.31
8.354	0.00	0.00	0.03	0.62	0.65	17.10	1.73
8.977	0.00	0.04	0.00	0.40	0.51	21.50	8.00
9.647	0.00	0.05	0.05	0.00	0.59	9.93	13.70
10.366	0.00	0.00	0.00	0.06	0.34	3.19	20.10
11.14	0.00	0.00	0.00	0.00	0.00	1.53	8.69
11.971	0.00	0.00	0.00	0.00	0.00	0.60	4.14
12.864	0.00	0.00	0.00	0.00	0.00	0.21	2.78
13.824	0.00	0.00	0.00	0.00	0.00	0.00	2.52
14.855	0.00	0.00	0.00	0.00	0.00	0.00	0.82

Table 9. Continued.

Nominal Particle Diameter, µm	**3**	**5**	**5**	**7**	**7**	**9**	**10**
Calculated Aerodynamic Diameter, µm	**3.11**	**4.97**	**4.88**	**7.33**	**7.10**	**9.04**	**9.87**
Size Distribution	**Mass Concentration, mg/m^3**						
15.963	0.00	0.00	0.00	0.00	0.00	0.20	0.41
17.154	0.00	0.00	0.00	0.00	0.00	0.00	0.00
18.434	0.00	0.00	0.00	0.00	0.00	0.00	0.00
19.81	0.00	0.39	0.00	0.00	0.00	0.00	0.00

Note: Particle sizes not mentioned above have mass concentration of 0 mg/m^3.

Table 10. Size distribution of particles of nominal sizes 10, 11, 13, 15, 17 µm generated from wind tunnel tests.

Nominal Particle Diameter, µm	**10**	**11**	**13**	**15**	**17**
Calculated Aerodynamic Diameter, µm	**9.79**	**10.83**	**13.05**	**15.07**	**17.24**
Size Distribution	**Mass Concentration, mg/m^3**				
6.264	0.01	0.00	0.00	0.00	0.00
6.732	0.05	0.03	0.02	0.00	0.00
7.234	0.10	0.00	0.00	0.00	0.00
7.774	0.31	0.05	0.00	0.02	0.00
8.354	3.28	0.29	0.03	0.00	0.00
8.977	9.56	1.56	0.04	0.04	0.00
9.647	13.50	6.45	0.18	0.09	0.00
10.366	14.70	13.20	0.56	0.17	0.00
11.14	6.39	27.90	4.93	0.28	0.00
11.971	2.24	25.80	14.10	0.78	0.00
12.864	0.43	6.85	17.30	4.28	0.11
13.824	0.27	3.32	42.00	10.40	0.13
14.855	0.17	0.82	27.20	19.10	2.14
15.963	0.00	0.61	7.57	55.60	8.18
17.154	0.00	0.00	4.82	27.90	13.40
18.434	0.00	0.00	1.89	6.30	25.50
19.81	0.00	0.00	0.00	6.25	20.70

Note: Sizes not mentioned above have mass concentration of 0 mg/m^3.

APPENDIX B

EXPECTED MASS CONCENTRATION OF AEROCET 831 AT WIND SPEED OF 2 KM/H

Table 11. Expected mass concentration for Aerocet 831 and ideal PM10 sampler at wind speed of 2 km/h.

Particle Size (um)	**Aerocet 831**			**Ideal PM10 Sampler**		
	Sampling Effectiveness	**Interval Mass Concentration (ug/m^3)**	**Expected Mass Concentration (ug/m^3)**	**Sampling Effectiveness**	**Interval Mass Concentration (ug/m^3)**	**Expected Mass Concentration (ug/m^3)**
(1)	(2)	(3)	(4)	(5)	(6)	(7)
<1.0	1	62.813	62.813	1	62.813	62.813
1.5	1	9.554	9.554	0.949	9.554	9.067
2	1	2.164	2.164	0.942	2.164	2.038
2.5	1	1.785	1.785	0.933	1.785	1.665
3	1	2.084	2.084	0.922	2.084	1.921
3.5	1	2.618	2.6179999	0.909	2.618	2.38
4	1.000000	3.211	3.2109996	0.893	3.211	2.867
4.5	0.999993	3.784	3.7839752	0.876	3.784	3.315
5	0.999838	4.3	4.2993033	0.857	4.3	3.685
5.5	0.998164	4.742	4.7332933	0.835	4.742	3.96
6	0.988543	5.105	5.0465109	0.812	5.105	4.145

Table 11. Continued.

Particle Size (um)	Aerocet 831			Ideal PM10 Sampler		
	Sampling Effectiveness	Interval Mass Concentration (ug/m^3)	Expected Mass Concentration (ug/m^3)	Sampling Effectiveness	Interval Mass Concentration (ug/m^3)	Expected Mass Concentration (ug/m^3)
(1)	(2)	(3)	(4)	(5)	(6)	(7)
6.5	0.954977	5.389	5.1463706	0.786	5.389	4.236
7	0.876656	5.601	4.9101507	0.759	5.601	4.251
7.5	0.744974	5.746	4.2806178	0.729	5.746	4.189
8	0.575870	5.834	3.3596253	0.697	5.834	4.066
8.5	0.402171	5.871	2.3611470	0.664	5.871	3.898
9	0.254083	5.864	1.4899400	0.628	5.864	3.683
9.5	0.146107	5.822	0.8506363	0.59	5.822	3.435
10	0.077113	5.75	0.4433975	0.551	5.75	3.168
10.5	0.037692	5.653	0.2130712	0.509	5.653	2.877
11	0.017213	8.257	0.1421289	0.465	8.257	3.84
12	0.003024	10.521	0.0318106	0.371	10.521	3.903
13	0.000442	9.902	0.0043788	0.269	9.902	2.664
14	0.000056	9.25	0.0005208	0.159	9.25	1.471
15	0.000006	8.593	5.554E-05	0.041	8.593	0.352
16	0.000001	7.948	5.460E-06	0	7.948	0
17	0.000000	7.329	5.059E-07	0	7.329	0

Table11. Continued.

Particle Size (um)	Aerocet 831			Ideal PM10 Sampler		
	Sampling Effectiveness	**Interval Mass Concentration (ug/m^3)**	**Expected Mass Concentration (ug/m^3)**	**Sampling Effectiveness**	**Interval Mass Concentration (ug/m^3)**	**Expected Mass Concentration (ug/m^3)**
(1)	(2)	(3)	(4)	(5)	(6)	(7)
18	6.66E-09	9.904	6.601E-08	0	9.904	0
20	5.78E-11	11.366	6.576E-10	0	11.366	0
22	4.83E-13	9.54	4.612E-12	0	9.54	0
24	4.10E-15	7.997	3.285E-14	0	7.997	0
26	0	6.704	0	0	6.704	0
28	0	5.627	0	0	5.627	0
30	0	7.785	0	0	7.785	0
35	0	7.8	0	0	7.8	0
40	0	5.192	0	0	5.192	0
45	0	4.959	0	0	4.959	0
		$C_{sam(exp)}$=	**125.326**		**$C_{ideal(exp)}$=**	**143.889**

APPENDIX C

EXPECTED MASS CONCENTRATION OF AEROCET 831 AT WIND SPEED OF 8 KM/H

Table 12. Expected mass concentration for Aerocet 831 and ideal PM10 sampler at wind speed of 8 km/h.

Particle Size (um)	**Aerocet 831**			**Ideal PM10 Sampler**		
	Sampling Effectiveness	**Interval Mass Concentration (ug/m^3)**	**Expected Mass Concentration (ug/m^3)**	**Sampling Effectiveness**	**Interval Mass Concentration (ug/m^3)**	**Expected Mass Concentration (ug/m^3)**
(1)	(2)	(3)	(4)	(5)	(6)	(7)
<1.0	1	62.813	62.813	1	62.813	62.813
1.5	1	9.554	9.554	0.949	9.554	9.067
2	1	2.164	2.164	0.942	2.164	2.038
2.5	1	1.785	1.785	0.933	1.785	1.665
3	1.000000	2.084	2.0840000	0.922	2.084	1.921
3.5	0.999999	2.618	2.6179966	0.909	2.618	2.38
4	0.999973	3.211	3.2109127	0.893	3.211	2.867
4.5	0.999722	3.784	3.7829489	0.876	3.784	3.315
5	0.998308	4.3	4.2927231	0.857	4.3	3.685
5.5	0.993020	4.742	4.7088995	0.835	4.742	3.96
6	0.978679	5.105	4.9961584	0.812	5.105	4.145

Table 12. Continued.

Particle Size (um)	Aerocet 831			Ideal PM10 Sampler		
	Sampling Effectiveness	Interval Mass Concentration (ug/m^3)	Expected Mass Concentration (ug/m^3)	Sampling Effectiveness	Interval Mass Concentration (ug/m^3)	Expected Mass Concentration (ug/m^3)
(1)	(2)	(3)	(4)	(5)	(6)	(7)
6.5	0.948519	5.389	5.1115702	0.786	5.389	4.236
7	0.896799	5.601	5.0229696	0.759	5.601	4.251
7.5	0.821662	5.746	4.7212695	0.729	5.746	4.189
8	0.726407	5.834	4.2378593	0.697	5.834	4.066
8.5	0.618536	5.871	3.6314251	0.664	5.871	3.898
9	0.507366	5.864	2.9751965	0.628	5.864	3.683
9.5	0.401529	5.822	2.3377002	0.59	5.822	3.435
10	0.307304	5.75	1.7669962	0.551	5.75	3.168
10.5	0.228069	5.653	1.2892722	0.509	5.653	2.877
11	0.164609	8.257	1.3591765	0.465	8.257	3.84
12	0.079749	10.521	0.8390437	0.371	10.521	3.903
13	0.035670	9.902	0.3532067	0.269	9.902	2.664
14	0.014986	9.25	0.1386250	0.159	9.25	1.471
15	0.005998	8.593	0.0515426	0.041	8.593	0.352
16	0.002313	7.948	0.0183838	0	7.948	0
17	0.000867	7.329	0.0063552	0	7.329	0

Table 12. Continued.

Particle Size (um)	Aerocet 831			Ideal PM10 Sampler		
	Sampling Effectiveness	**Interval Mass Concentration (ug/m^3)**	**Expected Mass Concentration (ug/m^3)**	**Sampling Effectiveness**	**Interval Mass Concentration (ug/m^3)**	**Expected Mass Concentration (ug/m^3)**
(1)	(2)	(3)	(4)	(5)	(6)	(7)
18	0.000318	9.904	0.0031527	0	9.904	0
20	4.11E-05	11.366	0.0004680	0	11.366	0
22	5.17E-06	9.54	4.938E-05	0	9.54	0
24	6.46E-07	7.997	5.172E-06	0	7.997	0
26	8.14E-08	6.704	5.462E-07	0	6.704	0
28	1.04E-08	5.627	5.879E-08	0	5.627	0
30	1.37E-09	7.785	1.068E-08	0	7.785	0
35	9.73E-12	7.8	7.595E-11	0	7.8	0
40	8.43E-14	5.192	4.380E-13	0	5.192	0
45	0	4.959	0	0	4.959	0
		$C_{sam(exp)}$=	**135.874**		**$C_{ideal(exp)}$ =**	**143.889**

APPENDIX D

EXPECTED MASS CONCENTRATION OF AEROCET 831 AT WIND SPEED OF 24 KM/H

Table 13. Expected mass concentration for Aerocet 831 and ideal PM10 sampler at wind speed of 24 km/h.

Particle Size (um)	**Aerocet 831**			**Ideal PM10 Sampler**		
	Sampling Effectiveness	**Interval Mass Concentration (ug/m^3)**	**Expected Mass Concentration (ug/m^3)**	**Sampling Effectiveness**	**Interval Mass Concentration (ug/m^3)**	**Expected Mass Concentration (ug/m^3)**
(1)	(2)	(3)	(4)	(5)	(6)	(7)
<1.0	1	62.813	62.813	1	62.813	62.813
1.5	1	9.554	9.554	0.949	9.554	9.067
2	1	2.164	2.164	0.942	2.164	2.038
2.5	1	1.785	1.785	0.933	1.785	1.665
3	1	2.084	2.084	0.922	2.084	1.921
3.5	1	2.618	2.618	0.909	2.618	2.38
4	1	3.211	3.211	0.893	3.211	2.867
4.5	1	3.784	3.7840000	0.876	3.784	3.315
5	1.000000	4.3	4.3000000	0.857	4.3	3.685
5.5	1.000000	4.742	4.7419985	0.835	4.742	3.96
6	0.999995	5.105	5.1049746	0.812	5.105	4.145

Table 13. Continued.

Particle Size (um)	Aerocet 831			Ideal PM10 Sampler		
	Sampling Effectiveness	Interval Mass Concentration (ug/m^3)	Expected Mass Concentration (ug/m^3)	Sampling Effectiveness	Interval Mass Concentration (ug/m^3)	Expected Mass Concentration (ug/m^3)
(1)	(2)	(3)	(4)	(5)	(6)	(7)
6.5	0.999952	5.389	5.3887421	0.786	5.389	4.236
7	0.999690	5.601	5.5992636	0.759	5.601	4.251
7.5	0.998546	5.746	5.7376428	0.729	5.746	4.189
8	0.994774	5.834	5.8035087	0.697	5.834	4.066
8.5	0.984959	5.871	5.7826953	0.664	5.871	3.898
9	0.964065	5.864	5.6532747	0.628	5.864	3.683
9.5	0.926585	5.822	5.3945758	0.59	5.822	3.435
10	0.868560	5.75	4.9942213	0.551	5.75	3.168
10.5	0.789465	5.653	4.4628479	0.509	5.653	2.877
11	0.692934	8.257	5.7215525	0.465	8.257	3.84
12	0.477010	10.521	5.0186234	0.371	10.521	3.903
13	0.282814	9.902	2.8004200	0.269	9.902	2.664
14	0.146164	9.25	1.3520204	0.159	9.25	1.471
15	0.066999	8.593	0.5757219	0.041	8.593	0.352
16	0.027730	7.948	0.2203988	0	7.948	0
17	0.010535	7.329	0.0772140	0	7.329	0

Table 13. Continued.

Particle Size (um)	Aerocet 831			Ideal PM10 Sampler		
	Sampling Effectiveness	**Interval Mass Concentration (ug/m^3)**	**Expected Mass Concentration (ug/m^3)**	**Sampling Effectiveness**	**Interval Mass Concentration (ug/m^3)**	**Expected Mass Concentration (ug/m^3)**
(1)	(2)	(3)	(4)	(5)	(6)	(7)
18	0.003728	9.904	0.0369187	0	9.904	0
20	0.000395	11.366	0.0044922	0	11.366	0
22	3.57E-05	9.54	0.0003406	0	9.54	0
24	2.90E-06	7.997	2.320E-05	0	7.997	0
26	2.20E-07	6.704	1.479E-06	0	6.704	0
28	1.61E-08	5.627	9.073E-08	0	5.627	0
30	1.15E-09	7.785	8.997E-09	0	7.785	0
35	1.58E-12	7.8	1.239E-11	0	7.8	0
40	2.44E-15	5.192	1.268E-14	0	5.192	0
45	0	4.959	0	0	4.959	0
		$C_{sam(exp)}$=	**166.784**		**$C_{ideal(exp)}$ =**	**143.889**